Acta Geophysica
https://doi.org/10.1007/s11600-024-01421-4

RESEARCH ARTICLE - ATMOSPHERIC & SPACE SCIENCES

# Fine structures of a solar type III radio bursts observed with LOFAR

**Bartosz Dabrowski[1] · Aleksandra Wolowska[1] · Christian Vocks[2] · Jasmina Magdalenić[3,4] · Peijin Zhang[5,6] · Pawel Flisek[1] · Malte Bröse[2,7] · Diana E. Morosan[8] · Andrzej Krankowski[1] · Adam Fron[1] · Gottfried Mann[2] · Pietro Zucca[9] · Mario Bisi[10] · Richard Fallows[10] · Peter Gallagher[11] · Christophe Marqué[4] · Barbara Matyjasiak[12] · Hanna Rothkaehl[12]**

Received: 22 January 2024 / Accepted: 13 June 2024


**Abstract**
We present spectral and imaging LOFAR (LOw-Frequency ARray) observations in the 20 – 40 MHz range of solar radio bursts fine structures, such as flag-like, sail-like, and dot-like that appeared on 8 April 2019. These structures were associated with type III solar radio bursts that occurred in the 40 – 80 MHz band. The mean duration and spectral widths of the fine structures range from 1.0 to 3.4 s and from 0.3 to 0.9 MHz, respectively. Additionally, we investigated the radio images of eight fine structures – two flags, two sails and four dots. This allowed us to determine their emission source sizes, which ranged from 240 to 392 arcmin$^2$, and their frequencies from 25.58 to 39.25 MHz as well as their location. They occurred on the east side of the Sun and were most likely associated with an emerging active region NOAA AR 12738, where a weak B1.7 flare was observed.

**Keywords** Sun · Radio · Bursts · Fine structures · Corona · LOFAR

## Introduction

Particularly important in the study of the processes that occur during solar flares are type III bursts (e.g. Wild and McCready 1950; Wild 1950a, b; Abranin et al. 1980; Melnik et al. 2011; Reid and Ratcliffe 2014; Melnik et al. 2021). In the dynamic spectrum they usually occur in groups (lasting a few minutes) of several almost vertical structures of enhanced radio emission. The duration of the individual structures in the metre wave range is up to a few seconds. The number of elements per group increases with frequency, and above 300 MHz it can reach

Edited by Prof. Iwona Stanisławska (ASSOCIATE EDITOR) / Prof. Theodore Karacostas (CO-EDITOR-IN-CHIEF).

✉ Bartosz Dabrowski
bartosz.dabrowski@uwm.edu.pl

1 Space Radio-Diagnostics Research Centre, University of Warmia and Mazury, R. Prawochenskiego 9, 10-719 Olsztyn, Poland

2 Leibniz-Institut für Astrophysik Potsdam, An der Sternwarte 16, D-14482 Potsdam, Germany

3 Center for mathematical Plasma Astrophysics, KU Leuven, 3001 Leuven, Belgium

4 Royal Observatory of Belgium, 1180 Ukkel, Brussels, Belgium

5 Center for Solar-Terrestrial Research, New Jersey Institute of Technology, Newark, NJ, USA

6 Cooperative Programs for the Advancement of Earth System Science, University Corporation for Atmospheric Research, Boulder, CO, USA

7 Zentrum für Astronomie und Astrophysik, Technische Universität Berlin, Hardenbergstraße 36, 10623 Berlin, Germany

8 Department of Physics and Astronomy, University of Turku, 20014 Turku, Finland

9 ASTRON – The Netherlands Institute for Radio Astronomy, Oude Hoogeveensedijk 4, 7991 PD Dwingeloo, The Netherlands

10 RAL Space, United Kingdom Research and Innovation - Science and Technology Facilities Council, Rutherford Appleton Laboratory, Harwell Campus, Oxfordshire OX11 0QX, UK

11 School of Cosmic Physics, Dublin Institute for Advanced Studies, 31 Fitzwilliam Place, Dublin 2 D02 PN40, Ireland

12 Space Research Center of the Polish Academy of Sciences, Bartycka 18a, 00-716 Warsaw, Poland

Published online: 13 August 2024

several hundred (Benz 2002). Type III bursts sometimes (on dynamic spectra) are observed as distinguishable pairs of fundamental and harmonic components (e.g. Wild et al. 1954; Melnik et al. 2018; Jebaraj et al. 2023a).

Another type of radio burst that can show a variety of fine structures are type IV bursts. These fine structures include spikes, pulsations, fibres and zebras, (e.g. Bernold 1980 and Melnik et al. 2008). Their study is crucial for a better understanding of the plasma processes occurring in the corona, as well as their diagnostics and verification of the obtained results with laboratory plasma studies (Chernov 2011). Fine structures of solar radio emission have been studied by various authors, e.g. Bhonsle et al. (1979), Magdalenić et al. (2006), Chernov et al. (2007), Magdalenić et al. (2020), Pulupa et al. (2020), Chen et al. (2021), Jebaraj et al. (2023b), and Zhang et al. (2024). Recently a new generation of radio telescopes such as, e.g., LOw Frequency ARray (LOFAR; van Haarlem et al. (2013)) has significantly improved the quality of radio observations of the Sun in terms of the coverage of the observed bandwidth, temporal and frequency resolution, sensitivity and, in the case of interferometers, also spatial resolution. This allowed detailed studies of fine structures.

Magdalenić et al. (2006) proposed a categorization for the supershort structures found in metric solar type IV radio bursts (200 – 600 MHz band) lasting between 4 to 60 ms. These structures were classified into three categories: (i) simple broadband, (ii) simple narrowband, and (iii) complex. Simple narrowband structures, characterized by a bandwidth smaller than 20 MHz, were further divided into spike-like and patch-like supershort structures. Of particular significance to our research are the patch-like bursts, which were further categorized as flag-like, sail-like, and dot-like bursts. Flag-like bursts, observed on dynamic spectra, exhibit symmetric frequency profiles and strongly asymmetric time profiles, with a steep profile in the rising phase of the burst. Sail-like bursts display a triangular shape, with symmetrical frequency profiles and asymmetric time profiles. Dot-like bursts are identified as increases in radio emissions, characterized by symmetric time and frequency profiles (Magdalenić et al. 2020). Figure 1 presents a schematic diagram illustrating the classification of solar radio fine structures.

In this paper, we present spectra and images of fine structures, such as flag-like, sail-like, and dot-like, observed with LOFAR in the 20 – 40 MHz range on 8 April 2019. These structures were associated with type III solar radio bursts that occurred in the 40 – 80 MHz band.

## Observations and data analysis

LOFAR is a radio interferometer situated in Europe, comprising 52 stations, with 38 stations in the Netherlands and the remaining 14 spread across several European countries: France, Germany, Ireland, Latvia, Poland, Sweden, and the United Kingdom. Within the Netherlands, the 38 LOFAR stations encompass 24 core stations (including six contributing to the "Superterp") and 14 remote stations. The International LOFAR Telescope (ILT) boasts its widest baselines reaching up to approximately 2000 km. Each LOFAR station conducts observations utilizing two kinds of antennas: the Low Band Antennas (LBA) functioning within the 10 to 90 MHz range and the High Band Antennas (HBA) operating between 110 and 240 MHz.

In our study, we utilized a segment of the data obtained from the LOFAR observation project LT10_002, titled "Advancing Space Weather Science with LOFAR and the Parker Solar Probe". This involved the integration of data from 36 LOFAR stations, comprising 24 core and 12 remote stations. Our research encompassed dynamic spectra and imaging observations within the frequency range of 20 to 80 MHz ("LBA Outer" configuration). These 36 stations possess a maximum baseline of approximately 76.1 km, enabling the creation of a radio image theoretically endowed with a spatial resolution of about 8.1 arcseconds at 80 MHz (van Haarlem et al. 2013). However, this resolution is constrained to about one arcminute due to coronal scattering effects (Mercier et al. 2015). To derive the stations' gains, we employed Taurus A as a calibrator in our analysis. The solar interferometric imaging is processed and visualized with lofarSun (Zhang et al. 2022). The dynamic spectra

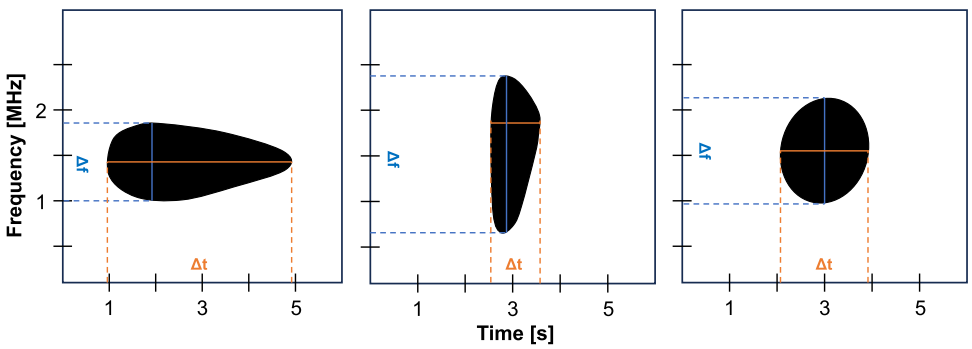


**Fig. 1** Schematic diagram shows the classification of solar radio fine structures flag-like (left panel), sail-like (middle panel), and dot-like (right panel). Structures of this type appear irregularly on the dynamic spectra. Duration and frequency band of selected fine structures are shown as $\Delta t$ and $\Delta f$, respectively

were prepared using the LOFAR Solar Imaging Pipeline developed at the Leibniz-Institut für Astrophysik Potsdam (Breitling et al. 2015).

The interferometric images of the fine structures were only taken at a single frequency, one image per structure. The reason for this approach was the very narrow bandwidth of the studied structures (0.2 to 3 MHz). Additionally, the data from which interferometric images were generated are recorded with an irregular frequency interval varying from 0.4 to 2.1 MHz. Therefore, it was not always possible to obtain an image of the examined structure exactly at its maximum at a given frequency.

In our study of the Sun we identified a series of type III solar radio bursts (occurred in the 40 – 80 MHz band) recorded with LOFAR on 8 April 2019 between 09:42:00 UT and 11:38:59.6 UT (Fig. 2, one minute part of dynamic spectrum). We were unable to record the beginning and end of the bursts because of the limited observing time. The studied type III bursts were observed within the type III storm observed from about 09:00 UT until about 15:30 UT (Nançay Decameter Array) and associated with fine structures such as flag-, sail-, and dot-like observed in 20 – 40 MHz range (Fig. 2). The structures occur in the whole studied period in a random manner in the dynamic spectrum.

The studied radio event was not associated with any strong flares. During the event GOES (Geostationary Operational Environmental Satellite) registered a weak B1.7 solar flare originating from active region NOAA AR 12738 at N06E72. The flare started at 09:49 UT, reached a maximum at 09:52 UT, and ended at 09:54 UT.

The dynamic spectra (L700909_SAP000_B000_S0_P000_bf) were prepared using the LOFAR Solar Imaging Pipeline developed at the Leibniz-Institut für Astrophysik Potsdam (Breitling et al. 2015). To obtain interferometric images of the fine structures we used the same procedure as in the work by Dabrowski et al. (2023).

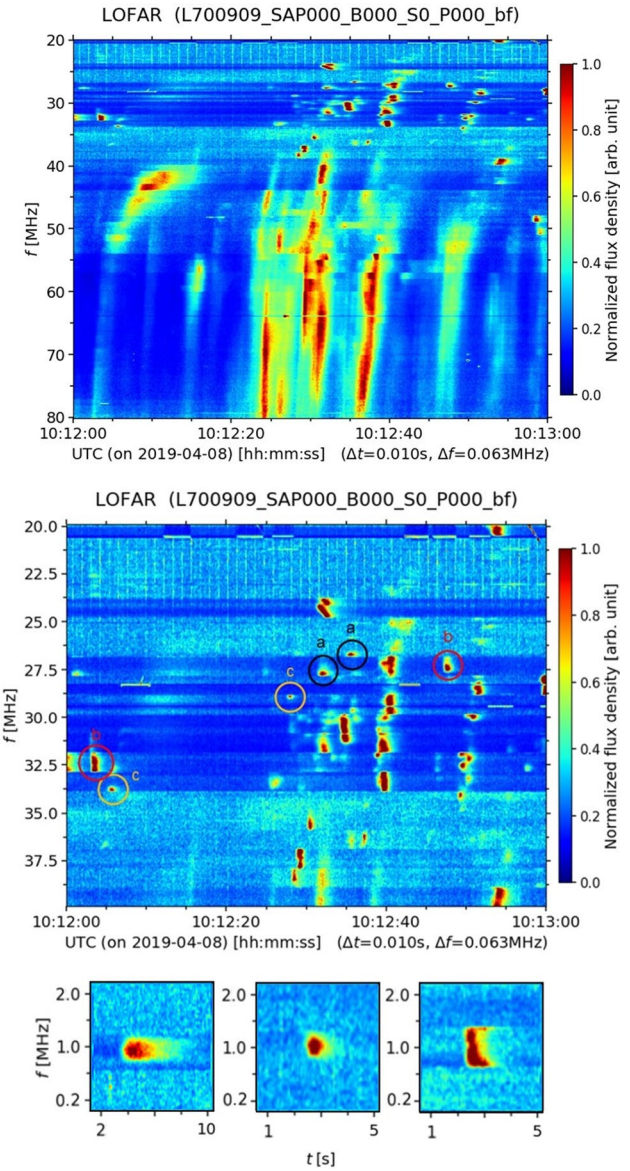


**Fig. 2** *Upper panel:* exemplary part of the solar dynamic spectrum with the series of the type III solar radio bursts in 40 – 80 MHz band recorded on 8 April 2019. It was accompanied by numerous fine structures in the 20 – 40 MHz band depicted in zoom in the *middle panel* with division to: **a** flag-like, **b** sail-like, and **c** dot-like structures (note that on the spectra the frequency axis is not continuous due to small gaps between subbands). In the *lower panel* are three examples of the discussed types of structures at high level of magnification: flag-like, dot-like and sail-like, respectively

## Classification of fine structures

The observed fine structures are morphologically similar to those described by Magdalenić et al. (2020) (and which were related to type II burst) and we will therefore apply the classification proposed there. During the type III bursts, we recorded such fine structures as (1) flag-like, (2) sail-like, and (3) dot-like.

We selected 24 flag-like, 12 sail-like and 21 dot-like fine structures for more detailed analysis (Table 1). These were well isolated structures, i.e., there were no other structures in their vicinity on the dynamic spectrum whose presence could affect the estimation of the parameters of the studied events. We determined the basic parameters of the fine structures, such as duration and spectral width (Fig. 1), within a constrained time and frequency range, revealing a detailed depiction of the studied phenomena and minimizing possible measurement errors. The obtained results are compared with those reported by Magdalenić et al. (2020), who investigated similar fine structures in the 10 – 190 MHz band (Table 1).

**Table 1** Basic parameters of the different fine structures. The results were compared with Magdalenić et al. (2020)

| Name | Flag-like | Sail-like | Dot-like |
|---|---|---|---|
| No. of events | 24 | 12 | 21 |
| Mean duration [s] | 3.4 | 1.1 | 1.0 |
| Duration $\Delta t$ [s] | 1.0 – 6.0 | 0.5 – 3.0 | 0.5 – 3.0 |
| Mean frequency band [MHz] | 0.3 | 0.9 | 0.5 |
| Frequency band $\Delta f$ [MHz] | 0.2 – 1.0 | 0.4 – 3.0 | 0.2 – 1.0 |
| Frequency range of occurrence [MHz] | 23.5 – 36.2 | 28.8 – 39.0 | 25.0 – 39.00 |
| Magdalenić et al. (2020) | | | |
| Duration $\Delta t$ [s] | 1.07 – 11.53 | 0.44 – 1.06 | 0.15 – 1.60 |
| Frequency band $\Delta f$ [MHz] | 0.09 – 1.00 | 0.71 – 1.62 | 0.16 – 0.88 |

The shortest time duration of the analysed flag-like structures was 1.0 s and the longest 6.0 s with the average of 3.4 s. In Magdalenić et al. (2020) the duration of this type of structure ranged from 1.07 to 11.53 s. Thus, its lower limit is comparable with our results, while its upper limit is twice as long as ours. As for the spectral width of the analysed flag-like structures, their average value is 0.3 MHz and the minimum and maximum values are 0.2 and 1.0 MHz, respectively. In Magdalenić et al. (2020) it is between 0.09 and 1.00 MHz and its lower limit is twice shorter than ours, while its upper limit is the same as our results. In general, the longer values of duration of the flag-like structures associated with type II bursts in comparison to type III seems consistent with the fact that electron beam velocity responsible for generating type III bursts is higher than in case of type II (Voshchepynets et al. 2015).

The shortest time duration of the analysed sail-like structures was 0.5 s and the longest 3.0 s with the average of 1.1 s. In Magdalenić et al. (2020) the duration of this type of structure ranged from 0.44 to 1.06 s. Thus, its lower limit is comparable to our results, while its upper limit is three times shorter than ours. As for the spectral width of the analysed sail-like structures, their average value is 0.9 MHz and the minimum and maximum values are 0.4 and 3.0 MHz, respectively. In Magdalenić et al. (2020) the frequency ranges from 0.71 to 1.62 MHz, with its lower limit being approximately twice as high as our results and its upper limit being half as high.

The shortest time duration of the analysed dot-like structures was 0.5 s and the longest 3.0 s with the average of 1.0 s. In Magdalenić et al. (2020) the duration of this type of structure ranged from 0.15 to 1.60 s. Thus, its lower limit is more than three times shorter than our results, while its upper limit is two times shorter than ours. As for the spectral width of the analysed dot-like structures, their average value is 0.5 MHz and the minimum and maximum values are 0.2 and 1.0 MHz, respectively. In Magdalenić et al. (2020) it is between 0.16 and 0.88 MHz and is similar to our results.

## Radio images of fine structures

We obtained radio images for eight fine structures, two for flag-like, two for sail-like and four for dot-like. The reason for difficulties in imaging this type of events are their narrowband nature and the fact that the acquired data are recorded with irregular frequency intervals ranging between 0.4 and 2.1 MHz.

In order to obtain interferometric images of the fine structures we determined the frequency and time corresponding to the maximum of the flux for each one. In the following step, the contour of the radio emission area is set to half of the maximum intensity. Additionally, for each contour a centroid is calculated (Table 2). Methodology is described in detail in Dabrowski et al. (2023).

From the radio images we found the sizes of the fine structure emission sources and their height in the solar corona (Table 2). To determine the heights of the structures, we used the well-known Newkirk radial electron density ($N_e$) model of the solar corona:

$$N_e = 4.2 \cdot 10^4 \cdot 10^{4.32/R}, \quad (1)$$

where $R$ is a distance from the centre of the Sun in units of the solar radius ($R_\odot$) (Newkirk 1961). The observed fine structures were situated between 1.63 and 1.89 $R_\odot$ from the solar centre, with an average altitude of 1.77 $R_\odot$.

The analysis showed that the eight studied fine structures occurred in different locations and frequencies (Table 2). Centroids of the fine structures were superimposed on the image of the Sun received in the AIA 171 Å channel by Solar Dynamics Observatory – SDO (Fig. 3). The observed fine structures occurred on the east side of the Sun and were most likely associated with an emerging active region NOAA AR 12738, where weak B1.7 flare was observed (the flare started at 09:49 UT, and ended at 09:54 UT).

The sizes of the emission sources in the investigated fine structures varied slightly, ranging from 288 to 372 arcmin$^2$ for flag-like structures (Fig. 4), 287 to 345 arcmin$^2$ for sail-like structures (Fig. 5), and 240 to 392 arcmin$^2$ for dot-like

**Table 2** Basic parameters of the studied fine structures observed on 8 April 2019 for which radio images were obtained

| Burst | Time [UT] | Freq [MHz] | Dur [s] | Freq. band [MHz] | $x$-axis[a] [arcsec] | $y$-axis[b] [arcsec] | Height[c] [$R_\odot$] | Size [arcmin$^2$] | Beam size [arcmin$^2$] |
|---|---|---|---|---|---|---|---|---|---|
| Flag-like | 11:22:20.5 | 25.58 | 6.0 | 0.4 | −1607 | 404 | 1.89 | 372 | 233 |
| Flag-like | 11:24:15.5 | 28.51 | 5.0 | 0.2 | −1204 | −464 | 1.81 | 288 | 201 |
| Sail-like | 10:53:26.8 | 28.51 | 0.5 | 0.4 | −1098 | 1434 | 1.81 | 345 | 188 |
| Sail-like | 11:36:35.2 | 39.25 | 0.5 | 0.4 | −1369 | 275 | 1.63 | 287 | 124 |
| Dot-like | 09:58:36.6 | 33.59 | 0.7 | 0.3 | −1752 | −118 | 1.71 | 269 | 210 |
| Dot-like | 10:01:46.2 | 31.44 | 2.0 | 0.8 | −1802 | −1168 | 1.75 | 240 | 163 |
| Dot-like | 10:02:56.6 | 33.59 | 1.0 | 0.3 | −1795 | −1125 | 1.71 | 392 | 267 |
| Dot-like | 10:53:29.0 | 27.53 | 1.0 | 0.3 | −1114 | 1547 | 1.84 | 331 | 199 |

[a]Location of the centroid in regard to the solar centre ($x$-axis)

[b]Location of the centroid in regard to the solar centre ($y$-axis)

[c]Height of emission source in regard to the solar centre

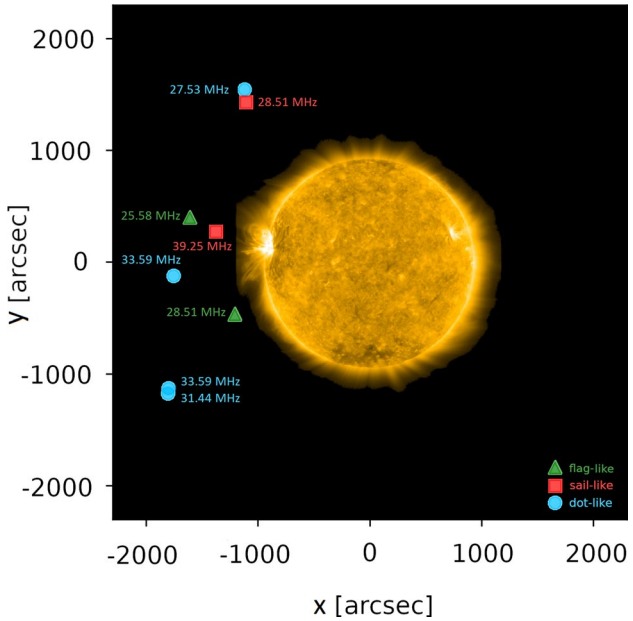


**Fig. 3** Image of the Sun received in the AIA 171 Å channel by SDO with superimposed centroids of the fine structures: flag-like (triangles), sail-like (squares), and dot-like (circles). The frequency at which they were obtained is shown next to the symbols

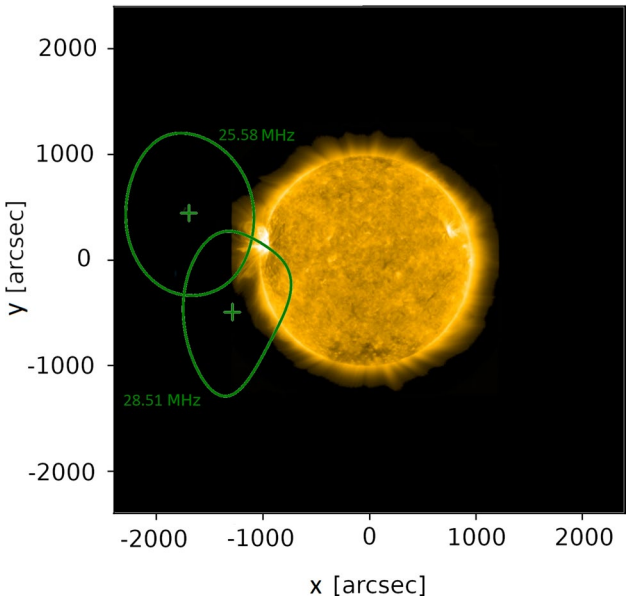


**Fig. 4** Image of the Sun received in the AIA 171 Å channel by SDO with superimposed radio contours showing the flag-like fine structures. The centroids of the areas are marked with a cross. The frequency at which they were obtained is shown next to the contours. Beam size for each contour can be shown in Table 2

structures (Fig. 6). Overall, the sizes of the fine structures were comparable across all studied cases. Importantly, the size of these structures did not show dependence on the frequency of observation. The telescope beam sizes were consistently 1.3 to 2.3 times smaller than those of the emission sources.

## Summary and discussion

We selected 57 fine structures for analysis and determined their basic parameters, such as duration and spectral width. Additionally, we obtained radio images for eight fine structures, two for flag-like, two for sail-like and four for dot-like.

We report fragmentation of the radio emission associated with type III radio bursts at lower frequencies observed in high time, frequency, and spatial resolution with LOFAR telescope. It appears that in the case of analysed event the fragmentation of the emission at low frequencies is much stronger than at higher frequencies. The density fluctuations determine the characteristics of the type III fine structures (Voshchepynets et al. (2015); Sishtla et al. (2023)). The main findings of our work are:

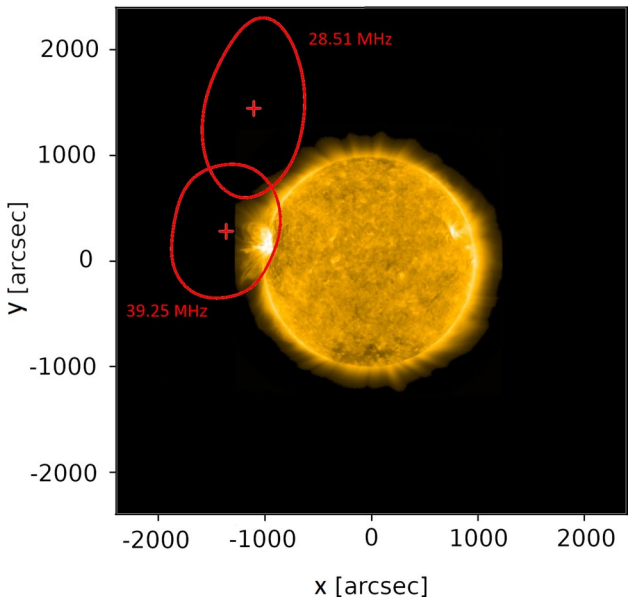


**Fig. 5** Image of the Sun received in the AIA 171 Å channel by SDO with superimposed radio contours showing the sail-like fine structures. The centroids of the areas are marked with a cross. The frequency at which they were obtained is shown next to the contours. Beam size for each contour can be shown in Table 2

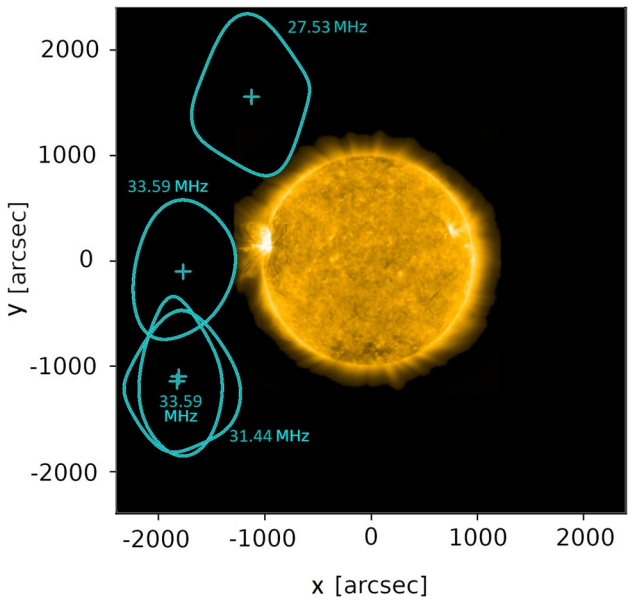


**Fig. 6** Image of the Sun received in the AIA 171 Å channel by SDO with superimposed radio contours showing the dot-like fine structures. The centroids of the areas are marked with a cross. The frequency at which they were obtained is shown next to the contours. Beam size for each contour can be shown in Table 2

1. We found fragmentation of the radio emission associated with type III bursts in 20 – 40 MHz band.
2. Several fine structures were noted that have been classified on the basis of their appearance on the dynamic spectrum according to the classification proposed by Magdalenić et al. (2020).
3. Coronal scattering can be one of the reasons having an influence on apparent positions of the sources of the studied fine structures. Dabrowski et al. (2023) estimated that the source observed at 35 MHz (roughly corresponding to the average frequency at which source sizes were studied, see Table 2) would be radially shifted by about 0.6 $R_{\odot}$ from its true location.
4. We observe identical fine structures in type III bursts as in type II bursts studied by Magdalenić et al. (2020). Therefore, this phenomenon appears to be universal, irrespective of the electron acceleration mechanism responsible for the bursts.

The analyses of fine structures carried out show that the LOFAR telescope is well suited for this type of task. Particularly relevant are the radio images of fine structures, which are relatively poorly studied in the literature at low frequencies (in the metric range).

**Acknowledgements** We acknowledge the National Science Centre, Poland and the Deutsche Forschungsgemeinschaft (DFG, German Research Foundation) for granting "LOFAR observations of the solar corona during Parker Solar Probe perihelion passages" in the Beethoven Classic 3 funding initiative under project numbers 2018/31/G/ST9/01341 and VO 2123/1-1, respectively. UWM would like to thank the Ministry of Education and Science of Poland for granting funds for the Polish contribution to the International LOFAR Telescope, LOFAR2.0 upgrade (decision number: 2021/WK/2) and for maintenance of the LOFAR PL-612 Bałdy station (decision number: 28/530020/SPUB/SP/2022). Diana E. Morosan acknowledges the Research Council of Finland project SolShocks (grant number: 354409). The authors thank the KSP "Solar Physics and Space Weather with LOFAR" team for support in solar LOFAR research. This paper is based on data obtained with the International LOFAR Telescope (ILT) under project code LT10_002. LOFAR (van Haarlem et al. 2013) is the Low Frequency Array designed and constructed by ASTRON. It has observing, data processing, and data storage facilities in several countries that are owned by various parties (each with their own funding sources), and that are collectively operated by the ILT foundation under a joint scientific policy. The ILT resources have benefited from the following recent major funding sources: CNRS-INSU, Observatoire de Paris and Université d'Orléans, France; BMBF, MIWF-NRW, MPG, Germany; Science Foundation Ireland (SFI), Department of Business, Enterprise and Innovation (DBEI), Ireland; NWO, The Netherlands; The Science and Technology Facilities Council, UK; Ministry of Science and Higher Education, Poland. The AIA data from SDO satellite are courtesy of NASA.

## Declaration

**Conflict of interest** On behalf of all authors, the corresponding author states that there is no Conflict of interest.

## References

Abranin EP, Bazelian LL, Goncharov NI et al (1980) Positions of solar storm burst sources by observations with a heliograph based on the UTR-2 antenna at 25 MHz. Solar Phys 66(2):393–409. https://doi.org/10.1007/BF00150593

Benz A (2002) Plasma Astrophysics. Kinetic Processes in Solar and Stellar Coronae, second edition 279. https://doi.org/10.1007/0-306-47719-X

Bernold T (1980) A catalogue of fine structures in type IV solar radio bursts. Astron Astrophys Suppl Ser 42:43–58

Bhonsle RV, Sawant HS, Degaonkar SS (1979) Exploration of the solar corona by high resolution solar decametric observations. Space Sci Rev 24(3):259–346. https://doi.org/10.1007/BF00212422

Breitling F, Mann G, Vocks C et al (2015) The LOFAR solar imaging pipeline and the LOFAR solar data center. Astron Comput 13:99–107. https://doi.org/10.1016/j.ascom.2015.08.001

Chen L, Ma B, Wu D et al (2021) An interplanetary type IIIb radio burst observed by parker solar probe and its emission mechanism. Astrophys J Lett 915(1):L22. https://doi.org/10.3847/2041-8213/ac0b43

Chernov GP (2011) Fine Structure of Solar Radio Bursts, vol 375. https://doi.org/10.1007/978-3-642-20015-1

Chernov GP, Stanislavsky AA, Konovalenko AA et al (2007) Fine structure of decametric type II radio bursts. Astron Lett 33(3):192–202. https://doi.org/10.1134/S1063773707030061

Dabrowski B, Mikuła K, Flisek P et al (2023) Interferometric imaging of the type IIIb and U radio bursts observed with LOFAR on 22 August 2017. Astron Astrophys 669:A52. https://doi.org/10.1051/0004-6361/202142905

Jebaraj IC, Krasnoselskikh V, Pulupa M et al (2023) Fundamental-harmonic pairs of interplanetary Type III radio bursts. Astrophys J Lett 955(1):L20. https://doi.org/10.3847/2041-8213/acf857

Jebaraj IC, Magdalenic J, Krasnoselskikh V et al (2023) Structured type III radio bursts observed in interplanetary space. Astron Astrophys 670:A20. https://doi.org/10.1051/0004-6361/202243494

Magdalenić J, Vršnak B, Zlobec P et al (2006) Classification and properties of supershort solar radio bursts. Astrophys J Lett 642(1):L77–L80. https://doi.org/10.1086/504521

Magdalenić J, Marqué C, Fallows RA et al (2020) Fine structure of a solar type II radio burst observed by LOFAR. Astrophys J Lett 897(1):L15. https://doi.org/10.3847/2041-8213/ab9abc

Melnik VN, Rucker HO, Konovalenko AA et al (2008) Solar Type IV bursts at frequencies 10–30 MHz. Nova Science Publishers, New York, pp 287–325

Melnik VN, Konovalenko AA, Rucker HO et al (2011) Observations of Powerful Type III bursts in the frequency range 10–30 MHz. Sol Phys 269(2):335–350. https://doi.org/10.1007/s11207-010-9703-4

Melnik VN, Brazhenko AI, Frantsuzenko AV et al (2018) Properties of decameter IIIb-III pairs. Sol Phys 293(2):26. https://doi.org/10.1007/s11207-017-1234-9

Melnik VN, Konovalenko AA, Dorovskyy VV et al (2021) Exploration of the solar decameter radio emission with the UTR-2 radio telescope. Radio Phys Radio Astron 26(1):74–89. https://doi.org/10.15407/rpra26.01.074

Mercier C, Subramanian P, Chambe G et al (2015) The structure of solar radio noise storms. Astron Astrophys 576:A136. https://doi.org/10.1051/0004-6361/201321064

Newkirk G (1961) The solar corona in active regions and the thermal origin of the slowly varying component of solar radio radiation. Astrophys J 133:983. https://doi.org/10.1086/147104

Pulupa M, Bale SD, Badman ST et al (2020) Statistics and polarization of type III radio bursts observed in the inner heliosphere. Astrophys J Suppl Ser 246(2):49. https://doi.org/10.3847/1538-4365/ab5dc0

Reid HAS, Ratcliffe H (2014) A review of solar type III radio bursts. Res Astron Astrophys 14(7):773–804. https://doi.org/10.1088/1674-4527/14/7/003

Sishtla CP, Jebaraj IC, Pomoell J et al (2023) The effect of the parametric decay instability on the morphology of coronal type III radio bursts. Astrophys J Lett 959(2):L33. https://doi.org/10.3847/2041-8213/ad137e

van Haarlem MP, Wise MW, Gunst AW et al (2013) LOFAR: the LOw-frequency ARray. Astron Astrophys 556:A2. https://doi.org/10.1051/0004-6361/201220873

Voshchepynets A, Krasnoselskikh V, Artemyev A et al (2015) Probabilistic model of beam-plasma interaction in randomly inhomogeneous plasma. Astrophys J 807(1):38. https://doi.org/10.1088/0004-637X/807/1/38

Wild JP (1950) Observations of the spectrum of high-intensity solar radiation at metre wavelengths. II. outbursts. Aust J Sci Res A Phys Sci 3(3):399–408. https://doi.org/10.1071/CH9500399

Wild JP (1950) Observations of the spectrum of high-intensity solar radiation at metre wavelengths. III. isolated bursts. Aust J Sci Res A Phys Sci 3:541. https://doi.org/10.1071/CH9500541

Wild JP, McCready LL (1950) Observations of the spectrum of high-intensity solar radiation at metre wavelengths. I. the apparatus and spectral types of solar burst observed. Aust J Sci Res A Phys Sci 3:387. https://doi.org/10.1071/CH9500387

Wild JP, Murray JD, Rowe WC (1954) Harmonics in the spectra of solar radio disturbances. Aust J Phys 7:439. https://doi.org/10.1071/PH540439

Zhang P, Zucca P, Kozarev K et al (2022) Imaging of the quiet sun in the frequency range of 20–80 MHz. Astrophys J 932(1):17. https://doi.org/10.3847/1538-4357/ac6b37

Zhang P, Morosan D, Kumari A et al (2024) Spatially resolved radio signatures of electron beams in a coronal shock. Astron Astrophys 683:A123. https://doi.org/10.1051/0004-6361/202347799